

# Constitutively-active Rheb mutants [T23M] and [E40K] drive increased production and secretion of recombinant protein in Chinese hamster ovary cells

Stuart De Poi<sup>1</sup>, Jianling Xie<sup>1</sup>, Christopher Mark Smales<sup>2</sup>, and Christopher Proud<sup>1</sup>

<sup>1</sup>South Australian Health and Medical Research Institute

<sup>2</sup>University of Kent

October 8, 2020

## Abstract

Monoclonal antibodies are high value agents used for disease therapy ('biologic drugs') or as diagnostic tools which are widely used in the health care sector. They are generally manufactured in mammalian cells, in particular Chinese hamster ovary (CHO) cells cultured in defined media, and are harvested from the medium. Rheb is a small GTPase which, when bound to GTP, activates mechanistic target of rapamycin complex 1 (mTORC1), a protein kinase that drives anabolic processes including protein synthesis and ribosome biogenesis. Here we show that certain constitutively-active mutants of Rheb drive faster protein synthesis in CHO cells and increase the expression of proteins involved in the processing of secreted proteins via the endoplasmic reticulum, which expands in response to expression of Rheb. Active Rheb mutants, in particular Rheb[T23M], drive increased cell number under serum-free conditions similar to those used in the biotechnology industry. Rheb[T23M] also enhances the expression of the reporter protein luciferase and, especially strongly, the secreted Gaussia luciferase. Moreover, Rheb[T23M] markedly (2-3 fold) enhances the amount of this luciferase and of a model immunoglobulin into the medium. Our data clearly demonstrate that expressing Rheb[T23M] in CHO cells provides a simple approach to promoting cell growth in defined medium and the production of secreted proteins of high commercial value

## Keywords

Recombinant proteins; biologic drug; mTORC1; defined medium; Rheb

## Introduction

Mammalian cell culture, most notably Chinese Hamster Ovary (CHO) cells, are commonly used to produce recombinant proteins such as monoclonal antibodies (mAbs) by the biopharmaceutical industry for use in both therapy and diagnosis (Goulet & Atkins, 2020). Such proteins offer enormous advances in disease therapy (or diagnosis) and are products of high commercial value. Over the last several decades there have been significant advances in the efficiency of CHO cells to produce these recombinant proteins (Budge et al., 2020; Kunert & Reinhart, 2016; Sharker & Rahman, 2020; Srirangan, Loignon, & Durocher, 2020). However, the rate of protein production remains a significant bottleneck, particularly for many of the novel format based biotherapeutics now in development, and therefore there remains substantial interest in further advancing the productivity of CHO cells (Budge et al., 2020; Sharker & Rahman, 2020).

The rate of protein synthesis (mRNA Translation) is one important limiting determinant of recombinant protein production (Godfrey et al., 2017; Khoo & Al-Rubeai, 2009; O'Callaghan et al., 2010; Roobol et al., 2020; Smales et al., 2004). One key regulator of protein synthesis is the mechanistic target of rapamycin complex 1 (mTORC1) (X. Wang & Proud, 2006). mTORC1 is a protein kinase that is activated by a variety of upstream signals, most notably amino acids (Kim, Goraksha-Hicks, Li, Neufeld, & Guan, 2008;

Sancak et al., 2008) and growth factors (Inoki, Li, Zhu, Wu, & Guan, 2002; B. D. Manning, Tee, Logsdon, Blenis, & Cantley, 2002), and acts as a master regulator of anabolic processes including protein synthesis (Proud, 2019) and ribosomal biogenesis (Iadevaia, Liu, & Proud, 2014; Saxton & Sabatini, 2017), both of which are critical for efficient protein production. This is achieved through phosphorylation of a number of downstream effectors such as ribosomal protein S6 kinase 1 (S6K1) (Chung, Kuo, Crabtree, & Blenis, 1992), eukaryotic elongation factor 2 kinase (eEF2K) (X. Wang et al., 2014), eIF4E binding protein 1 (4E-BP1) (Beretta, Gingras, Svitskin, Hall, & Sonenberg, 1996), and Maf1 (Michels et al., 2010), a regulator of ribosomal RNA transcription. mTORC1 signalling is thus potentially a major positive regulator of efficient, high-level production of recombinant proteins in mammalian cells. Increased phosphorylation of 4E-BP1, which permits increased translation initiation, has indeed been shown to increase production of interferon- $\gamma$  (Kaur et al., 2007). We have also previously shown that the ratio of eIF4E to 4E-BP1 correlates to higher cell productivity (Jossé, Xie, Proud, & Smales, 2016). In addition to this, mTORC1 drives other anabolic pathways that contribute to cell growth and faster protein production, including lipid synthesis (Caron, Richard, & Laplante, 2015) and ribosome biogenesis (Iadevaia et al., 2014).

mTORC1 is activated by the small GTPase Rheb (Ras homologue enriched in brain) when it is in its GTP-bound form; its conversion to the inactive GDP-bound state is promoted by the tuberous sclerosis complex which includes the proteins TSC1 and TSC2, the latter acting as a GTPase-activator protein (GAP) for Rheb (Garami et al., 2003; Inoki, Zhu, & Guan, 2003; Tee, Manning, Roux, Cantley, & Blenis, 2003). In turn, the ability of TSC1/2 to impair Rheb function is inhibited by signalling events activated by hormones, mitogenic stimuli and growth factors (Huang & Manning, 2008; Inoki et al., 2002; B.D. Manning & Cantley, 2003; Zhang et al., 2003). We have recently discovered that several mutants of Rheb (which occur in certain human cancers) are resistant to the GAP activity of TSC2 and are thus ‘constitutively active’, promoting high levels of mTORC1 activity in human cells (Jianling Xie et al., 2020).

The folding, assembly and maturation of most secreted proteins occurs, with the assistance of chaperones, within the endoplasmic reticulum (ER). Homeostatic control of the ER is mediated by the unfolded protein response (UPR) (Preissler & Ron, 2019). In response to protein disequilibrium in the ER, the protein kinase RNA-like ER kinase (PERK) undergoes homodimerization and becomes active (Cui, Li, Ron, & Sha, 2011). PERK then phosphorylates eukaryotic initiation factor 2 $\alpha$  (eIF2 $\alpha$ ) at serine-51 (Harding, Zhang, Bertolotti, Zeng, & Ron, 2000; Harding, Zhang, & Ron, 1999). eIF2 $\alpha$  is a component of the heterotrimeric initiation factor eIF2 which is required to deliver the initiator methionyl-tRNA to the 43S preinitiation complex in order to initiate mRNA translation (Merrick & Pavitt, 2018), a process that requires the hydrolysis of eIF2-bound GTP to GDP (Kapp & Lorsch, 2004). In order to facilitate subsequent initiation events, the guanine exchange factor (GEF) eIF2B binds eIF2 and catalyses the exchange of the GDP for GTP to regenerate active eIF2.GTP. When eIF2 $\alpha$  is phosphorylated in response to upstream stress, eIF2 is unable to be released from eIF2B and thus is no longer able to initiate translation (Bogorad, Lin, & Marintchev, 2018). This has two contrasting consequences which in combination mediate homeostasis of the ER. Firstly, it leads to global inhibition of protein synthesis, decreasing the ‘load’ of new proteins to be folded within the ER (Wek, 2018). However, secondly, certain mRNAs utilise their upstream open reading frames (uORFs) to undergo preferentially translation in response to P-eIF2 $\alpha$  mediated inhibition of general protein synthesis (Harding, Novoa, et al., 2000). One such protein is activating transcription factor 4 (ATF4). Translation of ATF4 is thus selectively upregulated in response to phosphorylation of eIF2 $\alpha$ . ATF4 is a transcription factor that drives the expression of genes responsible for protein homeostasis which are collectively called ER quality control genes (ERQC) (Preissler & Ron, 2019). ERQC genes consist mainly of chaperones and other protein folding genes; thus upregulation of ATF4 counters ER stress by increasing the protein folding capacity of the cell (Shaffer et al., 2004; Sriburi, Jackowski, Mori, & Brewer, 2004; M. Wang & Kaufman, 2016).

Here we show that two such Rheb mutants, T23M and E40K, drive constitutive mTORC1 signalling in CHO cells and enhance the production of recombinant protein including, importantly, its secretion from the cells. Manipulation of mTORC1 signalling by these Rheb mutants therefore has the clear potential to enhance the production of proteins of high commercial value.

## Materials and Methods

### *Cell Culture, Vectors and Transfection*

HEK293 cells were cultured in Dulbecco's modified Eagle medium (DMEM) containing 10% foetal bovine serum and 1% penicillin/streptomycin at 37°C with 5% (v/v) CO<sub>2</sub>. Firefly Luciferase (FLuc) and *Gaussia* Luciferase (GLuc) expressing Chinese Hamster Ovary (CHO) cells were cultured in Ham's F12 medium containing 10% foetal bovine serum and 1% penicillin/streptomycin at 37°C with 5% (v/v) CO<sub>2</sub>. EXPI-CHO cells were acquired from ThermoFisher Scientific (SA, Australia) and cultured in Expi-CHO Expression Medium. All cells were regularly tested for mycoplasma contamination. pRK7-FLAG-Rheb vectors were used as previously described (Jianling Xie et al., 2020). peGFP-N1 neomycin selection vector was a kind gift from Dr. Timothy Sargeant. To create stable transfection vectors, DNA sequence encoding FLAG-Rheb was amplified from pRK7-FLAG-Rheb vectors via PCR with the addition of 5' *EcoRI* and 3' *BamHI* restriction sites. Amplicons were cloned into peGFP-N1 neomycin selection vector via the *EcoRI* and *BamHI* restriction sites. Transfection into HEK293, FLuc-CHO and GLuc-CHO was performed using Lipofectamine 3000 (ThermoFisher Scientific, SA, Australia) according to the manufacturer's instructions. Transfections into EXPI-CHO was performed via the Expifectamine transfection system as per the manufacturer's instructions.

### *Immunofluorescence*

HEK293 cells were seeded into 2 cm x 1 cm chamber slides at a density of 50,000 cells/slide 24 h prior to transfection. Cells were grown until they reached 80% confluency. Medium was then removed, and cells washed 3x in PBS before being fixed in 1 mL of 4% (v/v) paraformaldehyde in PBS for 15 min. Cells were then washed 3x with PBS before being permeabilized with 1 mL of freshly made 0.05% (v/v) Triton X-100 in PBS for 5 min. Cells were washed 3x with PBS and blocked for 1 h in 10% (v/v) normal donkey serum. Cells were washed 3x with PBS before 400 µL of PBS containing 2% (v/v) normal donkey serum and 1/200 dilutions of indicated primary antibodies was added. Cells were left in primary antibody at 4°C overnight. Primary antibodies were removed, and cells washed 3x in PBS before secondary antibody solution of 400 µL PBS containing 2% (v/v) normal donkey serum and 1/200 dilutions of donkey anti-rabbit AF488, AF594 and AF647 were added to each sample. Cells were incubated under foil at room temperature for 1 h before secondary antibodies were removed and cells washed 3x with PBS. Cells were mounted with 400 µL of VectaShield Hardset containing DAPI and cover slips carefully applied. Cells were incubated overnight in a 5% (v/v) CO<sub>2</sub> incubator before being sealed with nail polish. Images were collected using a Leica TCS SP8X/MP (Leica Microsystems, NSW, Australia) confocal microscope and processed with ImageJ software package.

### *SUnSET Assay*

To perform surface sensing of translation (SUnSET) assays, cells were grown to 70-80% confluency in fully supplemented medium. Medium was then replaced for Earle's Balanced Salts Solution (EBSS). For one well, medium was replaced with EBSS containing 1 µM cycloheximide (CHX) as a positive control. After 30 min, puromycin was added to the cells to a final concentration of 1 µM and allowed to incorporate for 30 min. Cell lysates were then harvested for SDS-PAGE immunoblot analysis with detection of incorporated puromycin via an anti-puromycin antibody.

### *SDS-PAGE and Immunoblot Analysis*

SDS-PAGE/Western blot analysis was carried out as previously described (J. Xie et al., 2019). Briefly, cells were lysed in ice-cold lysis buffer containing 1% Triton X-100, 150 mM NaCl, 20 mM Tris-HCl pH 7.5, 2.5 mM sodium pyrophosphate, 1 mM EDTA, 1 mM EGTA, 1 mM sodium orthovanadate, 1 mM dithiothreitol (DTT) and 1 mM β-glycerophosphate supplemented with protease inhibitor cocktail. Protein concentrations were determined via Bradford assay and normalized. Equal aliquots of protein (20 µg) were denatured in Laemmli loading buffer, heated at 95°C for 3 min and separated by SDS-PAGE using gels containing 7-13% acrylamide and 0.1%-0.36% bis-acrylamide as required. Proteins were transferred to nitrocellulose membranes, which were blocked and incubated with primary antibody as indicated (Supplementary Table

S1). The relevant fluorescently-conjugated secondary antibody was applied and signals were imaged using a LiCor Odyssey® CLx imager (Millennium Science, VIC, Australia).

### *RT-qPCR*

Reverse transcription quantitative polymerase chain reaction (RT-qPCR) was performed by first extracting RNA via phenol-chloroform extraction using TriReagent (Sigma-Aldrich, NSW, Australia) as per the manufacturer's instructions (Jianling Xie et al., 2020). Contaminating DNA removal and reverse transcription were then performed on equal amounts of RNA using QuantiNova Reverse Transcription Kit. cDNA diluted 1:10 in nuclease free water was used as a template for qPCR reactions with SYBR Green PCR Master Mix (Sigma-Aldrich). For a list of primers used for qPCR reactions, see Supplementary Table S2.

### *Bromodeoxyuridine (BrdU) Assay*

Was performed as previously described (Jianling Xie et al., 2020). BrdU Cell Proliferation Assay Kit (Cell Signalling Technology, Danvers, MA #6813) was performed as per the manufacturer's instructions. Cells were plated at 10,000 cells per well in a 96-well plate 2 h prior to addition of 10  $\mu$ L of 10x BrdU solution. 2 h after addition of BrdU, cells were fixed/denatured for 30 min. BrdU detection antibody was diluted 1:100 and added to cells for 1 h. Cells were washed 3x in wash buffer before addition of HRP-linked secondary antibody for 30 min. Cells were washed 3x before addition of 3,3',5,5'-tetramethylbenzidine. After 30 min, STOP solution was added and absorbance determined at 450 nm.

### *Firefly and Gaussia Luciferase Assays*

Firefly luciferase assay was performed using Steady-Glo® Luciferase Assay System (Promega, NSW Sydney) as per the manufacturer's instructions. To prepare cells, FLuc-CHO cells were seeded in 6-well plates and transfected with vector encoding Rheb mutants. Cells were grown for 24 h and then seeded into 96-well plates. Cells were allowed to grow for 24 h before Firefly Luciferase assay was performed. 100  $\mu$ L of assay reagent was added to each well and 5 min allowed for cell lysis. Luminescence was then measured using GloMax® Discover microplate reader (Promega Australia, NSW, Australia)

*Gaussia* luciferase (GLuc) assays were performed using the BioLux® *Gaussia* Luciferase Assay Kit (New England Biolabs, Ipswich, MA) as per the manufacturer's instructions. Cells were prepared as per the Firefly luciferase assay. GLuc Assay solution was prepared by mixing 1:1000 BioLux® GLuc Substrate and BioLux® GLuc Assay buffer. 20  $\mu$ L of cell growth medium was transferred to a black 96-well plate and 50  $\mu$ L GLuc Assay solution added. Luminescence was read using a GloMax® Discover microplate reader with a 5 second integration.

### *Cell Growth Curves*

Cell growth curves were produced by seeding cells at a density of 1000 cells per well in 6-well plates. Cells were allowed to grow for 24 h before medium was replaced as indicated. Cells were counted on a haemocytometer every 24 h for 7 days. For GLuc-CHO cells, cells were counted every 4 h from 24 h post-seeding to 60 h post seeding.

### *IgG Production and Secretion Assay*

ExpiCHO-S cells stably expressing Rheb[WT], [T23M] or [E40K] were seeded at a density of  $4 \times 10^6$  cells/mL in 125 mL shaker flasks and allowed to grow for 16 h to a density of  $10 \times 10^6$  cells/mL. Cells were then diluted to  $6 \times 10^6$  cells/mL and transfected with pcDNA3.2 vector encoding heavy and light chains of rabbit IgG1 at 2:1 light:heavy chain ratio via ExpiFectamine CHO Transfection Kit according to the manufacturer's instructions. ExpiFectamine CHO/plasmid complexes were prepared by diluting 12  $\mu$ g plasmid in 1 mL OptiPRO medium and 80  $\mu$ L of ExpiFectamine CHO Reagent in 920  $\mu$ L OptiPRO medium. Diluted ExpiFectamine reagent was added to diluted DNA and incubated at room temperature for 5 min before ExpiFectamine CHO/DNA complex was added to cells. Cells were incubated at 37°C and 8% CO<sub>2</sub> on an orbital shaker at 125 rpm at 19 mm shaking diameter. After 24 h, 150  $\mu$ L of ExpiCHO Enhancer and 6 mL of ExpiCHO Feed were added to cells. 20  $\mu$ L of medium were removed each day in order to determine rate

of secretion. 10-days post transfection, cells were pelleted via centrifugation at 1000 rpm for 10 min and supernatant collected.

IgG concentration in growth medium was determined via Easy-Titre Rabbit IgG Assay Kit as per the manufacturer's instructions. Growth medium containing rabbit IgG1 were diluted 1:1000 in PBS. 20  $\mu$ L of Anti-IgG Sensitized Beads were transferred to a 96-well plate and 20  $\mu$ L of diluted cell medium containing rabbit IgG added. Plates were mixed on a plate mixer for 5 min before 100  $\mu$ L of blocking buffer was added to each well. Absorbance was measured at 405 nm and IgG concentration calculated from a standard curve of known IgG concentration generated from 1:2 serial dilutions starting at 500 ng/mL.

## Results

Rheb-T23M and E40K drive mild endoplasmic reticulum stress through increased protein synthesis

In a recent study (Jianling Xie et al., 2020), we showed that certain mutations in Rheb (which arise in human cancers) are able to drive hyperactive mTORC1 signalling in mouse or human cells.

As mTORC1 is well known to promote multiple steps in mRNA translation (protein synthesis), we assessed whether these Rheb mutants can drive increased protein synthesis. To do this we employed surface sensing of translation western blot assay (SUnSET-WB (Schmidt, Clavarino, Ceppi, & Pierre, 2009)). In the SUnSET-WB technique cells are treated with a low concentration of puromycin (1  $\mu$ M), a compound which acts as a structural analogue of aminoacyl-tRNA (specifically tyrosyl-tRNA) and can therefore be incorporated into nascent polypeptides. Incorporated puromycin can then be detected by western blot with puromycin-specific antibodies. Thus SUnSET-WB is a radioactive-free assay to measure rates of protein synthesis. For our initial experiments, we elected to utilise HEK293 cells as they are both a common cell line used for cell signalling studies, and ones in which we have previously shown Rheb mutations drive constitutive mTORC1 signalling. HEK293 cells transiently transfected with vectors encoding FLAG-Rheb[WT], [T23M], [Y35N] or [E40K] or an empty vector (EV) were transferred to Dulbecco's phosphate buffered saline (D-PBS) for 30 min prior to the addition of 1  $\mu$ M puromycin for an additional 30 min. One well of untransfected cells was pre-treated with 50  $\mu$ g/mL of cycloheximide, a potent inhibitor of protein synthesis, for 30 minutes prior to the addition of puromycin to provide a 'negative control' for any immunostaining that is not due to ongoing protein synthesis. Cell lysates were then harvested for western blot analysis. Rheb[T23M] and [E40K] each stimulated a large increase in puromycin incorporation compared to either Rheb[WT] or EV (Fig. 1a; quantified in Fig. 1b). Interestingly, despite Rheb[Y35N] being known to drive hyperactive mTORC1 signalling, it did not increase puromycin incorporation, in line with the fact that Rheb mutants differ in their downstream effects (Jianling Xie et al., 2020).

It has been shown that increases in overall protein synthesis can overload the protein folding capacity of the endoplasmic reticulum (ER) resulting in ER stress and activation of the unfolded protein response (Sriburi et al., 2004). This process has been observed in response to increased mTORC1 activity (Appenzeller-Herzog & Hall, 2012; Dong et al., 2015) and results in an expansion of the ER and therefore increased protein folding capacity (Shaffer et al., 2004; Sriburi et al., 2004; M. Wang & Kaufman, 2016). We hypothesised that Rheb-mutants may drive mild ER stress resulting in increased ER volume and protein folding capacity. To test this, we first studied several proteins involved in both the ATF4 arm of the UPR and proteins involved in protein folding. Cells stably expressing plasmids encoding Rheb[WT] or mutants of Rheb showed increased expression of ATF4 compared to the empty vector (Fig. 1c). Interestingly, there was no significantly greater change in ATF4 protein expression in cells expressing Rheb mutants compared to WT. However, Rheb[T23M] and [E40K] did promote an increase, or tended to cause an increase, in classical UPR markers or ER resident proteins including PERK, BiP/Grp78, IRE-1 $\alpha$ , PDI and ERO1-1 $\alpha$  (Fig. 1c; quantified in Supplementary Figure 1). Calnexin did not change. There was also an increase in the protein folding markers ERO1-L $\alpha$  (Fig. 1c; quantified in Supplementary Fig. S1).

To assess whether these changes reflected increased levels of the corresponding mRNAs, we performed RT-qPCR for the mRNAs encoding BiP (*HSPA5* ; Fig. 1d), PDI (*PDI* ; Fig. 1e), IRE1 $\alpha$  (*ERN1* ; Fig. 1f), and ATF4 (*ATF4* ; Fig. 1g) whose levels were increased by mutant Rheb expression. Increases in mRNA

encoding both UPR and protein folding proteins correlated with protein increases with the notable exception of ATF4 mRNA which was significantly higher in cells expressing Rheb mutants compared to both the EV and Rheb[WT] (Fig. 1d-g). To determine if these observed changes are associated with an increase in ER volume, we performed immunofluorescence on HEK293 cells stably expressing Rheb mutants or WT as well as an empty vector. To image the ER, we chose to probe with an anti-calnexin antibody as calnexin is an ER surface protein and there was no significant change in the level of calnexin protein with the different Rheb mutants (Fig. 1b) (so that any alterations seen in the extent of the ER would be independent of changes in its overall levels). Volume was calculated based on a  $\beta$ -actin counter stain. Both Rheb[T23M] and [E40K] promote a significant increase in ER volume compared to Rheb[WT] and EV. Rheb[Y35N] did not promote an increase in ER volume (Fig. 2a; quantified Fig.2b). These data suggest the Rheb[T23M] and [E40K] mutants can each promote increase protein synthesis which, in turn, drives a mild ER stress resulting in increased ER volume and concomitant protein folding capacity.

These data for HEK293 cells prompted us to extend our studies to CHO cells, the dominant type of cells used for in industry for producing recombinant proteins, particularly as an expanded ER is reported to enhance the ability of CHO cells to produce secretory recombinant proteins (Budge et al., 2020).

Rheb mutants drive constitutive mTORC1 signalling in CHO cells

Enabling cells to produce more protein is highly beneficial for the efficient production of therapeutic proteins such as monoclonal antibodies (mAbs). mAbs are most commonly produced from Chinese Hamster Ovary (CHO) cells (Kunert & Reinhart, 2016; Sharker & Rahman, 2020). Given that Rheb mutants increase protein synthesis and enhance ER capacity in HEK293 cells, we hypothesised that these mutants, when expressed in CHO cells, may also result in increased secretory mAb titres. For our initial experiments we utilised our previously reported CHO cell lines that stably expresses either the secreted luciferase reporter *Gaussia* Luciferase (GLuc) or Firefly Luciferase (FLuc). As it was first important to confirm that Rheb mutants can also drive hyperactive mTORC1 signalling in CHO cells, we co-transfected them with vectors encoding Rheb mutants and with vectors encoding FLAG-TSC1/2. Here we used both GLuc-CHO and FLuc-CHO cells grown in monolayer in fully supplemented Ham's F12 medium. Cells were then starved of serum for 16 h and then transferred to D-PBS for 1 h prior to lysates being harvested for immunoblot analysis. mTORC1 activity was assessed by monitoring the phosphorylation of the well-characterized mTORC1 substrate, S6K1, at Thr389, rpS6 at Ser240 and Ser244 (a substrate of S6K1) and of 4E-BP1 at Thr37, Thr46 and Ser65 (all direct substrates of mTORC1). Phosphorylation of all effectors were slightly elevated in cells expressing Rheb[WT] compared to cells that received EV and, as expected, was almost completely abolished in cells that were co-transfected with FLAG-TSC1/2 in both GLuc-CHO (Fig. 3a) and FLuc-CHO cells (Fig. 3b).

In contrast, cells expressing Rheb[T23M] or [E40K] showed higher levels of phosphorylation of S6K1, rpS6 and 4E-BP1, even in the presence of FLAG-TSC1/2, suggesting these mutants drive hyperactivation of mTORC1 (i.e., which is insensitive to inhibition by TSC) in GLuc-CHO (Fig. 3a) and FLuc-CHO (Fig. 3b) cells. These data are consistent with our findings for expression of these mutants of Rheb in human cells (Jianling Xie et al., 2020).

We next sought to determine the effect of Rheb mutations on cell proliferation. To do this, GLuc-CHO cells were allowed to proliferate for 7 days while being counted on a haemocytometer every day in order to generate a cell growth curve. None of the Rheb mutants had any effect on cell proliferation when GLuc-CHO cells were grown in fully supplemented medium or medium supplemented with 0.5% FBS (Fig. 3c, Supplementary Fig. S2a). However, when GLuc-CHO cells were grown in medium supplemented with 1% FBS, Rheb[T23M] promoted both an increased rate of proliferation as well as supporting an increased total cell number (Supplementary Fig. S2b). This was even more pronounced when cells were grown in the absence of FBS with Rheb[T23M] promoting a marked increase in the rate of proliferation (Fig. 3d). To confirm these results, BrdU incorporation assays were performed in order to more directly quantify the effect of Rheb[T23M] on cell proliferation. Consistent with our findings for HEK293 cells (Jianling Xie et al., 2020), Rheb[T23M], [Y35N] and [E40K] each drove increased cell proliferation in both GLuc-CHO and FLuc-CHO cells compared to both Rheb[WT] and EV (Fig. 3e/f).

Rheb[T23M] and [E40K] drive increased protein synthesis and secretion dependent on ER stress

To test whether Rheb mutants drive an increase in recombinant protein production in CHO cells, we transfected FLuc-CHO cells with vectors encoding Rheb mutants and performed firefly luciferase assays every 48 h for 7 days. In order to determine if the protein production capacity of *individual* cells was increased (and to take into account possible differences in cell number due to the effect of Rheb mutants on cell proliferation), the firefly luciferase assays were normalised to the number of cells present as counted on a haemocytometer. Cells expressing Rheb[T23M] showed a small yet significant increase in Firefly luciferase (Fig. 4a/b) indicating an increase in protein production. Interestingly, other Rheb mutants did not significantly increase the accumulation of firefly luciferase suggesting that while they promote constitutive mTORC1 activity, this does not result in universal upregulation of protein production.

Next, we sought to determine the effect of Rheb mutants on the output of a secreted protein, which is the key parameter for the production of recombinant proteins of commercial interest, which are harvested from the culture medium. To do this, we transfected GLuc-CHO cells with vectors encoding Rheb mutants and performed *Gaussia* luciferase assays on the growth media. As with the firefly luciferase assays, results were normalised to cell number to give an indication of accumulated *Gaussia* luciferase secretion on a per-cell basis. In contrast to firefly luciferase production, Rheb[T23M], [Y35N] and [E40K] all promoted a significant increase in GLuc secretion as calculated in this way (Fig. 4c). Cells expressing these mutants showed an approximately 3-fold increase in GLuc secretion after 7 days; no difference was seen in amounts of intracellular GLuc (not shown), consistent with Rheb mutants boosting secretion of the additional GLuc. As expected, treatment with the potent mTOR inhibitor AZD8055 (Chresta et al., 2010) reversed the effect of mutant Rheb (Fig. 4c/d). These data suggest that, as well as increasing protein synthesis, Rheb mutants may also increase cells' secretory capacity, consistent with the findings for HEK293 cells. As increased ER volume is known to increase secretory capacity (Budge et al., 2020; M. Wang & Kaufman, 2016), we also performed the GLuc assay using cells treated with a combination of the ER stress response inhibitors iPERK (Axten et al., 2012), a compound that inhibits the kinase activity of PERK, and ISRIB (Sidrauski et al., 2013), a compound that interferes with the ability of phosphorylated eIF2 to inhibit the guanine exchange of eIF2B (Sidrauski, McGeachy, Ingolia, & Walter, 2015). Inhibition of the ER stress response dramatically decreased the secretion of GLuc from cells expressing Rheb mutants (Fig. 4e) indicating Rheb mediated ER expansion is crucial for increased GLuc secretion. Consistent with this, western blot analysis of GLuc-CHO cells transiently expressing Rheb mutants or an empty vector show that Rheb[T23M] and [E40K] significantly drive increased expression of the ATF4 arm of the UPR (Fig. 4f).

Rheb[T23M] and [E40K] drive increased mAb secretion under conditions similar to those used in industry

While GLuc-CHO cells act as a good reporter system for interrogating the effect of Rheb mutants on protein secretion, there are several limitations that make these cells unsuitable for use as an industrial research tool. First, to be useful in an industrial context, CHO cells must be grown in suspension and in chemically defined, serum-free media. Second, while GLuc may be a secreted protein, it is not a model biotherapeutic protein and lacks glycosylation. To address these issues, we acquired EXPI-CHO cells and modified them to stably express Rheb[WT], [T23M], [Y35N] or [E40K] (Supplementary Fig. S3). We then performed SDS-PAGE western blot analysis on lysates harvested from these cells to confirm the hyperactivity of mTORC1 signalling and ER stress phenotype observed in HEK293 and GLuc-CHO cells was present in these cells. Consistent with GLuc-CHO cells, in EXPI-CHO cells stably expressing Rheb mutants or Rheb[WT], [T23M] and [E40K] drove increased phosphorylation of rpS6 at Ser240/244, indicative of activated mTORC1, as well as increased phosphorylation of 4E-BP1 at Thr37 and Thr46 suggesting that Rheb[T23M] and [E40K] drive hyperactive mTORC1 signalling in these cells (Fig. 5a).

In addition, Rheb[T23M] and [E40K] each drove increased expression of the ATF4 arm of the UPR as well as of ER stress markers such as BiP (Fig. 5b). Interestingly, we were unable to detect any differences in protein synthesis via SUNSET assay (Fig. 5c). This is likely because these cells stably express Rheb mutants and therefore increased protein synthesis likely results in increased total protein amounts. As the amounts of cell lysate loaded onto the immunoblot gels are normalised to total protein, such normalisation will effectively

‘eliminate’ any effect on the rate of protein synthesis. Cells expressing Rheb[T23M] or [E40K] also showed significantly faster cell proliferation as assessed by counting cells on a haemocytometer every 24 h for 7 days (Fig. 5d) as well as in a BrdU assay for DNA synthesis (Fig. 5e)

To determine the effect of Rheb mutants on mAb production and secretion in these cells, we transfected cells with a vector encoding the heavy and light chains of rabbit IgG1 and grew the cells in serum-free, chemically-defined medium for 10 days with the cells being fed on day 2. This more closely mimics the type of conditions the biopharmaceutical industry would use when using a transient expression approach and CHO cells to produce a recombinant IgG. We found that after 10 days of growth, Rheb[T23M] and [E40K] promoted a 2-3 fold increase in IgG1 yield (Fig. 5f). Testing accumulated antibody in the growth medium every 24 h over the course of the experiment revealed that duration of antibody secretion was similar in all cases, but that the rate of release of secreted IgG1 was markedly increased in cells expressing Rheb[T23M] or [E40K]. This suggests that Rheb[T23M] and [E40K] promote both increased production and, very importantly, secretion of a recombinant antibody.

## Discussion

It is clear that any increase in IgG titre in medium is beneficial to the biopharmaceutical industry in terms of enhancing the production of the desired product and particularly its levels in the cell medium from which is it harvested. Here we show that Rheb mutations we previously identified are capable of increasing IgG titres in CHO cells grown in suspension in chemically-defined, serum-free medium replicating industrial growth conditions.

Consistent with our previous study (Jianling Xie et al., 2020), we found that the exogenous expression of the Rheb mutants Rheb[T23M], [Y35N] and [E40K] drive constitutive mTORC1 signalling through insensitivity to TSC-GAP activity and thus rendering mTORC1 insensitive to removal of upstream activators. We show that in HEK293 cells, Rheb[T23M] and [E40K] drive an increased rate of protein synthesis consistent with previous studies (Jianling Xie et al., 2020) as well as the known function of mTORC1 as a key regulator of protein synthesis (Proud, 2019) and ribosome biogenesis (Iadevaia et al., 2014). mTORC1 also promotes mitochondrial function (de la Cruz López, Toledo Guzmán, Sánchez, & García Carrancá, 2019). A recent paper has also shown the mTORC1 signaling can stimulate ATF4 expression independently of the UPR and thereby upregulate a subset of ATF4 target genes (Torrence et al., 2020). As a key activator of mTORC1 signalling, the expression of an active Rheb mutant such as T23M can drive multiple anabolic pathways, so that this single manipulation can lead to enhanced cell growth and proliferation and faster protein synthesis. This obviates the need to modify multiple genes thereby offering a substantial advantage for cell engineering.

We unexpectedly found that Rheb[Y35N], despite driving constitutive mTORC1 signalling, did not increase protein synthesis. This is consistent with our finding that, while Rheb[T23M] and [E40K] increased the levels of ATF4, Rheb[Y35N] did not. Rheb[T23M] and [E40K] also resulted in an increase in markers of the integrated stress response and expansion of the endoplasmic reticulum (ER).

These data suggest that the increase in protein synthesis driven by constitutive activation of mTORC1 increases the protein folding load on the ER. As unfolded proteins accumulate in the ER, the integrated stress response becomes activated; in the short term, this drives increased expression of proteins required for protein folding and expansion of the ER. If this expansion is enough to accommodate the increased protein folding requirements, cells can maintain increased protein synthesis without progressing into apoptosis which can occur during prolonged activation of the UPR (Shaffer et al., 2004; Sriburi et al., 2004; M. Wang & Kaufman, 2016). This mechanism allows cells to produce more protein without adverse effects. The fact we only observe this phenomenon in cells expressing Rheb[T23M] and [E40K] but not Rheb[Y35N] is surprising and suggests that mTORC1 activation alone is not sufficient to support a long-term increase in protein synthesis. We previously showed through proteomic analysis of NIH3T3 cells stably expressing Rheb[T23M] and [E40K] that additional pathways are activated by these mutations. Cells expressing Rheb[T23M] showed increased reliance on anaerobic glycolysis while cells expressing Rheb[E40K] showed increased autophagic flux (Jianling Xie et al., 2020). It is possible that activation of these pathways does not occur in Rheb[Y35N]



so that cells expressing Rheb[Y35N] are not able to sustain the energy or nutrient requirements to sustain prolonged increases in protein synthesis.

We show that this mechanism of mTORC1-driven activation of the UPR is required for increased secretion of the reporter *Gaussia*luciferase from CHO cells stably expressing GLuc when grown in monolayer. This hypothesis is supported by the observation that both inhibition of mTOR and inhibition of the ATF4 arm of the UPR decreased GLuc secretion. We also observed a significant upregulation of ATF4 in cells expressing Rheb[T23M] or [E40K]. We show that this is also true for CHO cells grown in suspension in chemically-defined, serum-free medium. We found that stable expression of Rheb[T23M] or [E40K] resulted in around a 2-3 fold increase in IgG1 secretion compared to Rheb[WT] overexpression or cells expressing only their endogenous Rheb.

These results clearly point to a potential approach to significant increasing the efficiency of production of commercially valuable proteins. A further development of this approach would be to generate cell lines stably expressing Rheb[T23M] or with the chromosomal copies of the Rheb gene mutated appropriately. Since all cells in the population would then be expressing mutant Rheb which is not the case for transient transfection), an even greater augmentation of protein output would be expected. The ability to double product output over the same time-frame without increasing nutrient input promises to make production of currently expensive treatments more efficient and may therefore lead to significant reductions in the cost of treatment, thus allowing more people being able to benefit from these highly effective treatments and/or at a lower cost. Our findings may thus be of direct value to the burgeoning ‘biological drug’ sector.

## Acknowledgements

Our initial studies in the UK were supported by Project Grants from the UK Biotechnology & Biological Sciences Research Council (BB/J007714/1 to CGP and BB/J006408/1 to CMS). Subsequent financial support was provided by the South Australian Health & Medical Research Institute, SDP gratefully acknowledges funding through the [Australian] Research Training Program.

## References

- Appenzeller-Herzog, C., & Hall, M. N. (2012). Bidirectional crosstalk between endoplasmic reticulum stress and mTOR signaling. *Trends in Cell Biology*, *22* , 274-282. doi:10.1016/j.tcb.2012.02.006
- Axten, J. M., Medina, J. R., Feng, Y., Shu, A., Romeril, S. P., Grant, S. W., . . . Gampe, R. T. (2012). Discovery of 7-methyl-5-(1-([3-(trifluoromethyl)phenyl]acetyl)-2,3-dihydro-1H-indol-5-yl)-7H-pyrrolo[2,3-d]pyrimidin-4-amine (GSK2606414), a potent and selective first-in-class inhibitor of protein kinase R (PKR)-like endoplasmic reticulum kinase (PERK). *Journal of Medicinal Chemistry*, *55* , 7193-7207. doi:10.1021/jm300713s
- Beretta, L., Gingras, A. C., Svitkin, Y. V., Hall, M. N., & Sonenberg, N. (1996). Rapamycin blocks the phosphorylation of 4E-BP1 and inhibits cap-dependent initiation of translation. *The EMBO Journal*, *15* , 658-664. doi:10.1002/j.1460-2075.1996.tb00398.x
- Bogorad, A. M., Lin, K. Y., & Marintchev, A. (2018). eIF2B Mechanisms of Action and Regulation: A Thermodynamic View. *Biochemistry*, *57* , 1426-1435. doi:10.1021/acs.biochem.7b00957
- Budge, J. D., Knight, T. J., Povey, J., Roobol, J., Brown, I. R., Singh, G., . . . Smales, C. M. (2020). Engineering of Chinese hamster ovary cell lipid metabolism results in an expanded ER and enhanced recombinant biotherapeutic protein production. *Metabolic Engineering*, *57* , 203-216. doi:10.1016/j.ymben.2019.11.007
- Caron, A., Richard, D., & Laplante, M. (2015). The Roles of mTOR Complexes in Lipid Metabolism. *Annual Review of Nutrition*, *35* , 321-348. doi:10.1146/annurev-nutr-071714-034355
- Chresta, C. M., Davies, B. R., Hickson, I., Harding, T., Cosulich, S., Critchlow, S. E., . . . Pass, M. (2010). AZD8055 is a potent, selective, and orally bioavailable ATP-competitive mammalian target of rapamycin

kinase inhibitor with in vitro and in vivo antitumor activity. *Cancer Research*, 70 , 288-298. doi:10.1158/0008-5472.CAN-09-1751

Chung, J., Kuo, C. J., Crabtree, G. R., & Blenis, J. (1992). Rapamycin-FKBP specifically blocks growth-dependent activation of and signaling by the 70 kd S6 protein kinases. *Cell*, 69 , 1227-1236. doi:10.1016/0092-8674(92)90643-q

Cui, W., Li, J., Ron, D., & Sha, B. (2011). The structure of the PERK kinase domain suggests the mechanism for its activation. *Acta Crystallogr D Biol Crystallogr*, 67 , 423-428. doi:10.1107/s0907444911006445

de la Cruz López, K. G., Toledo Guzmán, M. E., Sánchez, E. O., & García Carrancá, A. (2019). mTORC1 as a Regulator of Mitochondrial Functions and a Therapeutic Target in Cancer. *Frontiers in Oncology*, 9 , 1373. doi:10.3389/fonc.2019.01373

Dong, G., Liu, Y., Zhang, L., Huang, S., Ding, H. F., & Dong, Z. (2015). mTOR contributes to ER stress and associated apoptosis in renal tubular cells. *American Journal of Physiology-Renal Physiology*, 308 , F267-274. doi:10.1152/ajprenal.00629.2014

Garami, A., Zwartkruis, F. J., Nobukuni, T., Joaquin, M., Roccio, M., Stocker, H., . . . Thomas, G. (2003). Insulin activation of Rheb, a mediator of mTOR/S6K/4E-BP signaling, is inhibited by TSC1 and 2. *Molecular Cell*, 11 , 1457-1466. doi:10.1016/s1097-2765(03)00220-x

Godfrey, C. L., Mead, E. J., Daramola, O., Dunn, S., Hatton, D., Field, R., . . . Smales, C. M. (2017). Polysome profiling of mAb producing CHO cell lines links translational control of cell proliferation and recombinant mRNA loading onto ribosomes with global and recombinant protein synthesis. *Biotechnology Journal*, 12 . doi:10.1002/biot.201700177

Goulet, D. R., & Atkins, W. M. (2020). Considerations for the Design of Antibody-Based Therapeutics. *Journal of Pharmaceutical Sciences*, 109 , 74-103. doi:10.1016/j.xphs.2019.05.031

Harding, H. P., Novoa, I., Zhang, Y., Zeng, H., Wek, R., Schapira, M., & Ron, D. (2000). Regulated translation initiation controls stress-induced gene expression in mammalian cells. *Molecular Cell*, 6 , 1099-1108. doi:10.1016/s1097-2765(00)00108-8

Harding, H. P., Zhang, Y., Bertolotti, A., Zeng, H., & Ron, D. (2000). Perk is essential for translational regulation and cell survival during the unfolded protein response. *Molecular Cell*, 5 , 897-904. doi:10.1016/s1097-2765(00)80330-5

Harding, H. P., Zhang, Y., & Ron, D. (1999). Protein translation and folding are coupled by an endoplasmic-reticulum-resident kinase. *Nature*, 397 , 271-274. doi:10.1038/16729

Huang, J., & Manning, B. D. (2008). The TSC1-TSC2 complex: a molecular switchboard controlling cell growth. *Biochemical Journal*, 412 , 179-190. doi:10.1042/BJ20080281

Iadevaia, V., Liu, R., & Proud, C. G. (2014). mTORC1 signaling controls multiple steps in ribosome biogenesis. *Seminars in Cell and Developmental Biology*, 36 , 113-120. doi:10.1016/j.semcdb.2014.08.004

Inoki, K., Li, Y., Zhu, T., Wu, J., & Guan, K. L. (2002). TSC2 is phosphorylated and inhibited by Akt and suppresses mTOR signalling. *Nature Cell Biology*, 4 , 648-657. doi:10.1038/ncb839

Inoki, K., Zhu, T., & Guan, K. L. (2003). TSC2 mediates cellular energy response to control cell growth and survival. *Cell*, 115 , 577-590. doi:10.1016/s0092-8674(03)00929-2

Jossé, L., Xie, J., Proud, C. G., & Smales, C. M. (2016). mTORC1 signalling and eIF4E/4E-BP1 translation initiation factor stoichiometry influence recombinant protein productivity from GS-CHOK1 cells. *Biochemical Journal*, 473 , 4651-4664. doi:10.1042/bcj20160845

Kapp, L. D., & Lorsch, J. R. (2004). GTP-dependent recognition of the methionine moiety on initiator tRNA by translation factor eIF2. *Journal of Molecular Biology*, 335 , 923-936. doi:10.1016/j.jmb.2003.11.025

- Kaur, S., Lal, L., Sassano, A., Majchrzak-Kita, B., Srikanth, M., Baker, D. P., . . . Platanias, L. C. (2007). Regulatory effects of mammalian target of rapamycin-activated pathways in type I and II interferon signaling. *The Journal of Biological Chemistry*, *282* , 1757-1768. doi:10.1074/jbc.M607365200
- Khoo, S. H. G., & Al-Rubeai, M. (2009). Detailed understanding of enhanced specific antibody productivity in NS0 myeloma cells. *Biotechnology and Bioengineering*, *102* , 188-199. doi:10.1002/bit.22041
- Kim, E., Goraksha-Hicks, P., Li, L., Neufeld, T. P., & Guan, K. L. (2008). Regulation of TORC1 by Rag GTPases in nutrient response. *Nature Cell Biology*, *10* , 935-945. doi:10.1038/ncb1753
- Kunert, R., & Reinhart, D. (2016). Advances in recombinant antibody manufacturing. *Applied Microbiology and Biotechnology*, *100* , 3451-3461. doi:10.1007/s00253-016-7388-9
- Manning, B. D., & Cantley, L. C. (2003). Rheb fills a GAP between TSC and TOR. *Trends in Biochemical Sciences*, *28* , 573-576. doi:10.1016/j.tibs.2003.09.003
- Manning, B. D., Tee, A. R., Logsdon, M. N., Blenis, J., & Cantley, L. C. (2002). Identification of the tuberous sclerosis complex-2 tumor suppressor gene product tuberlin as a target of the phosphoinositide 3-kinase/akt pathway. *Molecular Cell*, *10* , 151-162. doi:10.1016/s1097-2765(02)00568-3
- Merrick, W. C., & Pavitt, G. D. (2018). Protein Synthesis Initiation in Eukaryotic Cells. *Cold Spring Harbor perspectives in biology*, *10* (12). doi:10.1101/cshperspect.a033092. (Accession No. 29735639)
- Michels, A. A., Robitaille, A. M., Buczynski-Ruchonnet, D., Hodroj, W., Reina, J. H., Hall, M. N., & Hernandez, N. (2010). mTORC1 directly phosphorylates and regulates human MAF1. *Molecular and Cellular Biology*, *30* , 3749-3757. doi:10.1128/mcb.00319-10
- O'Callaghan, P. M., McLeod, J., Pybus, L. P., Lovelady, C. S., Wilkinson, S. J., Racher, A. J., . . . James, D. C. (2010). Cell line-specific control of recombinant monoclonal antibody production by CHO cells. *Biotechnol and Bioengineering*, *106* , 938-951. doi:10.1002/bit.22769
- Preissler, S., & Ron, D. (2019). Early Events in the Endoplasmic Reticulum Unfolded Protein Response. *Cold Spring Harbor Perspectives in Biology*, *11* . doi:10.1101/cshperspect.a033894
- Proud, C. G. (2019). Phosphorylation and Signal Transduction Pathways in Translational Control. *Cold Spring Harbor perspectives in biology*, *11* (7). doi:10.1101/cshperspect.a033050. (Accession No. 29959191)
- Roobol, A., Roobol, J., Smith, M. E., Carden, M. J., Hershey, J. W. B., Willis, A. E., & Smales, C. M. (2020). Engineered transient and stable overexpression of translation factors eIF3i and eIF3c in CHOK1 and HEK293 cells gives enhanced cell growth associated with increased c-Myc expression and increased recombinant protein synthesis. *Metabolic Engineering*, *59* , 98-105. doi:10.1016/j.ymben.2020.02.001
- Sancak, Y., Peterson, T. R., Shaul, Y. D., Lindquist, R. A., Thoreen, C. C., Bar-Peled, L., & Sabatini, D. M. (2008). The Rag GTPases bind raptor and mediate amino acid signaling to mTORC1. *Science*, *320* , 1469-1501. doi:10.1126/science.1157535
- Saxton, R. A., & Sabatini, D. M. (2017). mTOR Signaling in Growth, Metabolism, and Disease. *Cell*, *168* , 960-976. doi:10.1016/j.cell.2017.02.004
- Schmidt, E. K., Clavarino, G., Ceppi, M., & Pierre, P. (2009). SUNSET, a nonradioactive method to monitor protein synthesis. *Nature Methods*, *6* , 275-277. doi:10.1038/nmeth.1314
- Shaffer, A. L., Shapiro-Shelef, M., Iwakoshi, N. N., Lee, A. H., Qian, S. B., Zhao, H., . . . Staudt, L. M. (2004). XBP1, downstream of Blimp-1, expands the secretory apparatus and other organelles, and increases protein synthesis in plasma cell differentiation. *Immunity*, *21* , 81-93. doi:10.1016/j.immuni.2004.06.010
- Sharker, S. M., & Rahman, M. A. (2020). Review of the current methods of Chinese Hamster Ovary (CHO) cells cultivation for production of therapeutic protein. *Current Drug Discovery Technology* . doi:10.2174/1570163817666200312102137

- Sidrauski, C., Acosta-Alvear, D., Khoutorsky, A., Vedantham, P., Hearn, B. R., Li, H., . . . Walter, P. (2013). Pharmacological brake-release of mRNA translation enhances cognitive memory. *eLife*, *2* , e00498. doi:10.7554/eLife.00498
- Sidrauski, C., McGeachy, A. M., Ingolia, N. T., & Walter, P. (2015). The small molecule ISRIB reverses the effects of eIF2 $\alpha$  phosphorylation on translation and stress granule assembly. *eLife*, *4* . doi:10.7554/eLife.05033
- Smales, C. M., Dinnis, D. M., Stansfield, S. H., Alete, D., Sage, E. A., Birch, J. R., . . . James, D. C. (2004). Comparative proteomic analysis of GS-NS0 murine myeloma cell lines with varying recombinant monoclonal antibody production rate. *Biotechnol and Bioengineering*, *88* , 474-488. doi:10.1002/bit.20272
- Sriburi, R., Jackowski, S., Mori, K., & Brewer, J. W. (2004). XBP1: a link between the unfolded protein response, lipid biosynthesis, and biogenesis of the endoplasmic reticulum. *Journal of Cell Biology*, *167* , 35-41. doi:10.1083/jcb.200406136
- Srirangan, K., Loignon, M., & Durocher, Y. (2020). The use of site-specific recombination and cassette exchange technologies for monoclonal antibody production in Chinese Hamster ovary cells: retrospective analysis and future directions. *Critical Reviews in Biotechnology*, *40* , 833-851. doi:10.1080/07388551.2020.1768043
- Tee, A. R., Manning, B. D., Roux, P. P., Cantley, L. C., & Blenis, J. (2003). Tuberous sclerosis complex gene products, Tuberin and Hamartin, control mTOR signaling by acting as a GTPase-activating protein complex toward Rheb. *Current Biology*, *13* , 1259-1268. doi:10.1016/s0960-9822(03)00506-2
- Torrence, M. E., MacArthur, M. R., Hosios, A. M., Valvezan, A. J., Asara, J. M., Mitchell, J. R., & Manning, B. D. (2020). The mTORC1-mediated activation of ATF4 promotes protein and glutathione synthesis downstream of growth signals. *bioRxiv* , 2020.2010.2003.324186. doi:10.1101/2020.10.03.324186
- Wang, M., & Kaufman, R. J. (2016). Protein misfolding in the endoplasmic reticulum as a conduit to human disease. *Nature*, *529* , 326-335. doi:10.1038/nature17041
- Wang, X., & Proud, C. G. (2006). The mTOR pathway in the control of protein synthesis. *Physiology (Bethesda)*, *21* , 362-369. doi:10.1152/physiol.00024.2006
- Wang, X., Regufe da Mota, S., Liu, R., Moore, C. E., Xie, J., Lanucara, F., . . . Proud, C. G. (2014). Eukaryotic elongation factor 2 kinase activity is controlled by multiple inputs from oncogenic signaling. *Molecular and Cellular Biology*, *34* , 4088-4103. doi:10.1128/mcb.01035-14
- Wek, R. C. (2018). Role of eIF2 $\alpha$  Kinases in Translational Control and Adaptation to Cellular Stress. *Cold Spring Harbor perspectives in biology*, *10* , a032870. doi:10.1101/cshperspect.a032870
- Xie, J., De Poi, S. P., Humphrey, S. J., Hein, L. K., Brunning, J. B., Pan, W., . . . Proud, C. G. (2020). TSC-Insensitive Rheb Mutations Induce Oncogenic Transformation Through a Combination of Constitutively Active mTORC1 Signalling and Metabolic Reprogramming. *BioRxiv* , 2020.2009.2007.284661.
- Xie, J., de Souza Alves, V., von der Haar, T., O'Keefe, L., Lenchine, R. V., Jensen, K. B., . . . Proud, C. G. (2019). Regulation of the Elongation Phase of Protein Synthesis Enhances Translation Accuracy and Modulates Lifespan. *Current Biology*, *29* , 737-749 e735. doi:10.1016/j.cub.2019.01.029
- Zhang, Y., Gao, X., Saucedo, L. J., Ru, B., Edgar, B. A., & Pan, D. (2003). Rheb is a direct target of the tuberous sclerosis tumour suppressor proteins. *Nature Cell Biology*, *5* , 578-581. doi:10.1038/ncb999

**Figure 1: Overexpression of Rheb promotes protein synthesis and increases ER stress markers.**  
**(A)** HEK293 cells were transfected with indicated vectors (EV = empty vector) and grown for 48 h prior to harvest. Lysates were harvested for SDS-PAGE western blot analysis with the indicated antibodies. SuNSET assays were then performed; the growth medium was changed for EBSS 90 min prior to addition of 30  $\mu$ M puromycin for 30 min. Samples indicated 'CHX' were pre-treated with cycloheximide, to inhibit ongoing protein synthesis. **(B)** Quantification of data from (A). **(C)** Lysates of cells that had been transfected

with the indicated vectors were analysed by SDS-PAGE and immunoblot using the indicated antibodies. **(D-G)** RT-qPCR analysis for known ER stress markers was performed on cDNA extracted from HEK293 cells expressing the indicated Rheb mutants or an empty vector (EV). Figures represent mean  $\pm$  s.d for 3 independent experiments. All graphs represent mean  $\pm$  s.d for 3 independent experiments. The data were analysed via Student's t-test compared to EV. \*:  $P < 0.05$ ; \*\*:  $P < 0.01$ ; \*\*\*  $P < 0.001$ .

**Figure 2: Rheb-T23M and E40K drive increased ER volume.** **(A)** Immunofluorescence of HEK293 cells transiently expressing the indicated Rheb mutants or EV. Cells were transfected with indicated vectors 24 h prior to fixation and addition of the indicated primary antibodies. **(B)** Quantification of **(A)** for the ratio of area containing Calnexin : area containing actin. Graph represent mean  $\pm$  s.d for 3 independent experiments. The data were analysed via Student's t-test. \*:  $P < 0.05$ ; \*\*  $P < 0.01$ .

**Figure 3: Rheb mutants drive constitutive mTORC1 signalling in GLuc-CHO cells.** **(A)** SDS-PAGE and western blot analysis of lysates harvested from GLuc-CHO cells transiently expressing the indicated Rheb mutants or transfected with an empty vector (EV); some were co-transfected with FLAG-TSC1/2, as indicated. The growth medium was replaced with medium lacking FBS for 16 h followed by D-PBS for 60 min immediately prior to harvesting. **(B)** As in **(A)** for FLuc-CHO cells. **(C)** GLuc-CHO cells expressing the indicated Rheb mutants or an empty vector (EV) were grown in fully supplemented media with cell number recorded every 24 h for 7 days. **(D)** As in **(C)** with cells grown in media lacking FBS. Figures are representative of mean  $\pm$  S.D for 3 independent experiments. **(E)** BrdU incorporation assay of FLuc-CHO cells expressing the indicated Rheb mutants or EV. Cells were allowed to grow in fully supplemented media for 24 h before addition of BrdU for 1 h. **(F)** As in **(E)** for GLuc-CHO cells. All graphs represent mean  $\pm$  s.d for 3 independent experiments. The data were analysed via Student's t-test compared to EV. \*:  $P < 0.05$ ; \*\*\*  $P < 0.001$ .

**Figure 4: Rheb mutants promote increased secretion of Gaussia Luciferase.** **(A)** CHO cells stably expressing Firefly luciferase (FLuc) were transfected with the indicated Rheb mutants or an empty vector (EV); FLuc assays were then performed every 48 h for 7 days. Results are normalized to cell number. **(B)** Quantification of data in **(A)** for day 7. **(C)** CHO cells stably expressing Gaussia Luciferase (GLuc) were transfected with the indicated Rheb mutants or an empty vector (EV) and treated with either DMSO (solid line) or 1  $\mu$ M AZD8055 (dashed line) for the duration of the experiment. GLuc assays performed on growth media every 48 h for 7 days. Results are normalized to cell number. **(D)** Quantification of data in **(C)** for day 7. **(E)** As in **(C)**, but cells were treated with a cocktail of 1  $\mu$ M iPERK and 1  $\mu$ M ISRIB (dashed line). Experiments shown **(C)** and **(E)** were performed simultaneously but are presented separately for clarity. **(F)** SDS-PAGE western blot analysis of cell lysates harvested from GLuc-CHO cells transiently transfected with the indicated Rheb mutants or an empty vector (EV). All graphs represent mean  $\pm$  s.d for 3 independent experiments. The data were analysed via Student's t-test. \*:  $P < 0.05$ ; \*\*  $P < 0.01$ ; \*\*\*  $P < 0.001$ .

**Figure 5: Rheb T23M and E40K drive increased secretion of mAb from CHO-S cells.** **(A)** SDS-PAGE western blot analysis of lysates harvested from Expi-CHO cells stably over-expressing the indicated Rheb mutant or transfected with empty vector (EV). **(B)** SDS-PAGE western blot analysis of lysates harvested from Expi-CHO cells stably over-expressing the indicated Rheb mutant or transfected with empty vector (EV). **(C)** EXPI-CHO cells stably expressing the indicated Rheb mutant or endogenous Rheb (Endo) were grown for 48 h prior treatment with 30  $\mu$ M puromycin for 30 m. Lysates were then harvested for SuNSET assays. **(D)** Expi-CHO cells stably expressing the indicated Rheb mutants or endogenous Rheb (Endo) were allowed to proliferate with cell number recorded every 24 h for 7 days. **(E)** BrdU incorporation assay of Expi-CHO cells stably expressing the indicated Rheb mutants or endogenous Rheb (Endo). Cells were allowed to proliferate for 24 h before addition of BrdU for 1 h. **(F)** IgG yield from Expi-CHO cells stably expressing the indicated Rheb mutant or endogenous Rheb after 10 days of expression. **(G)** Time course of IgG secretion from Expi-CHO cells stably expressing the indicated Rheb mutant. Figure represents n=1. All other figures are representative of 3 independent experiments. All graphs represent mean  $\pm$  s.d for 3 independent experiments. The data were analysed via Student's t-test compared to Endo. \*:  $P < 0.05$ ; \*\*  $P < 0.01$ ; \*\*\*  $P < 0.001$ .

**Supplementary Figure 1: Mutant Rheb drives an increase in levels of proteins of the ER stress response . Related to Figure 1**Quantification of SDS-PAGE western blot data for Fig. 1a. All graphs represent mean  $\pm$  s.d for 3 independent experiments. The data were analysed via Student's t-test compared to Endo. \*:  $P < 0.05$ .

**Supplementary Figure 2: Rheb-T23M displays increased proliferation on media containing reduced FBS. Related to Figure 3.** (A)GLuc-CHO cells expressing the indicated Rheb mutants or an empty vector (EV) were grown in media supplemented with 1% FBS with cell number recorded every 24 h for 7 days. (B) f-CHO cells expressing the indicated Rheb mutants or EV were grown in media supplemented with 0.5% FBS with cell number recorded every 24 h for 7 days. All graphs represent mean  $\pm$  s.d for 3 independent experiments. The data were analysed via Student's t-test compared to Endo. \*\*\*  $P < 0.001$ .

**Supplementary Figure 3: Characterization of Expi-CHO cells stably over expressing Rheb mutants. Related to Figure 5.** Sanger sequencing results of Expi-CHO monoclonal cell lines transfected with vector encoding both the indicated Rheb mutant and NeoR to grant resistance to G-418. Cells were grown for 6 weeks in the presence of 1  $\mu$ M G-418 before DNA was extracted and sequenced using primers specific to the inserted plasmid.

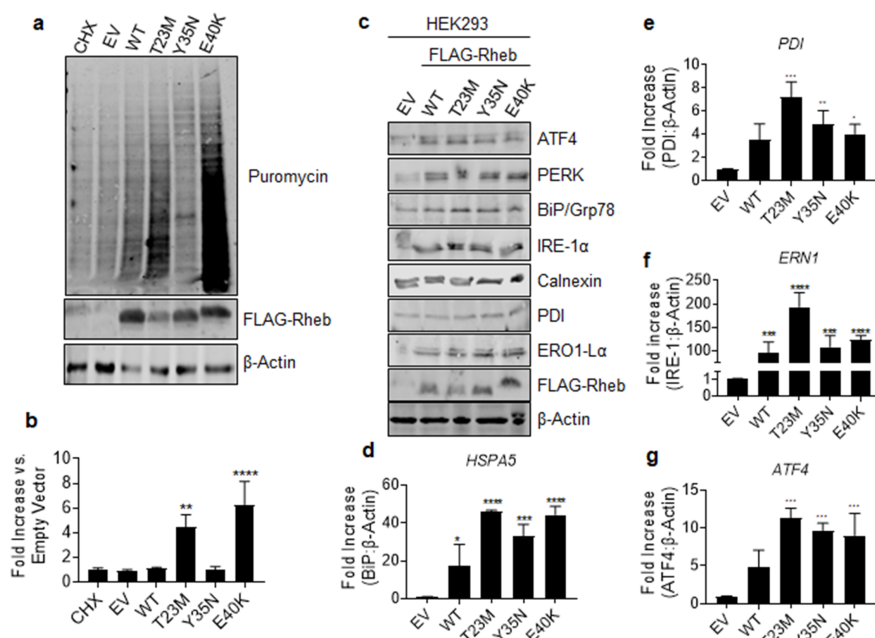


**Figure 1**

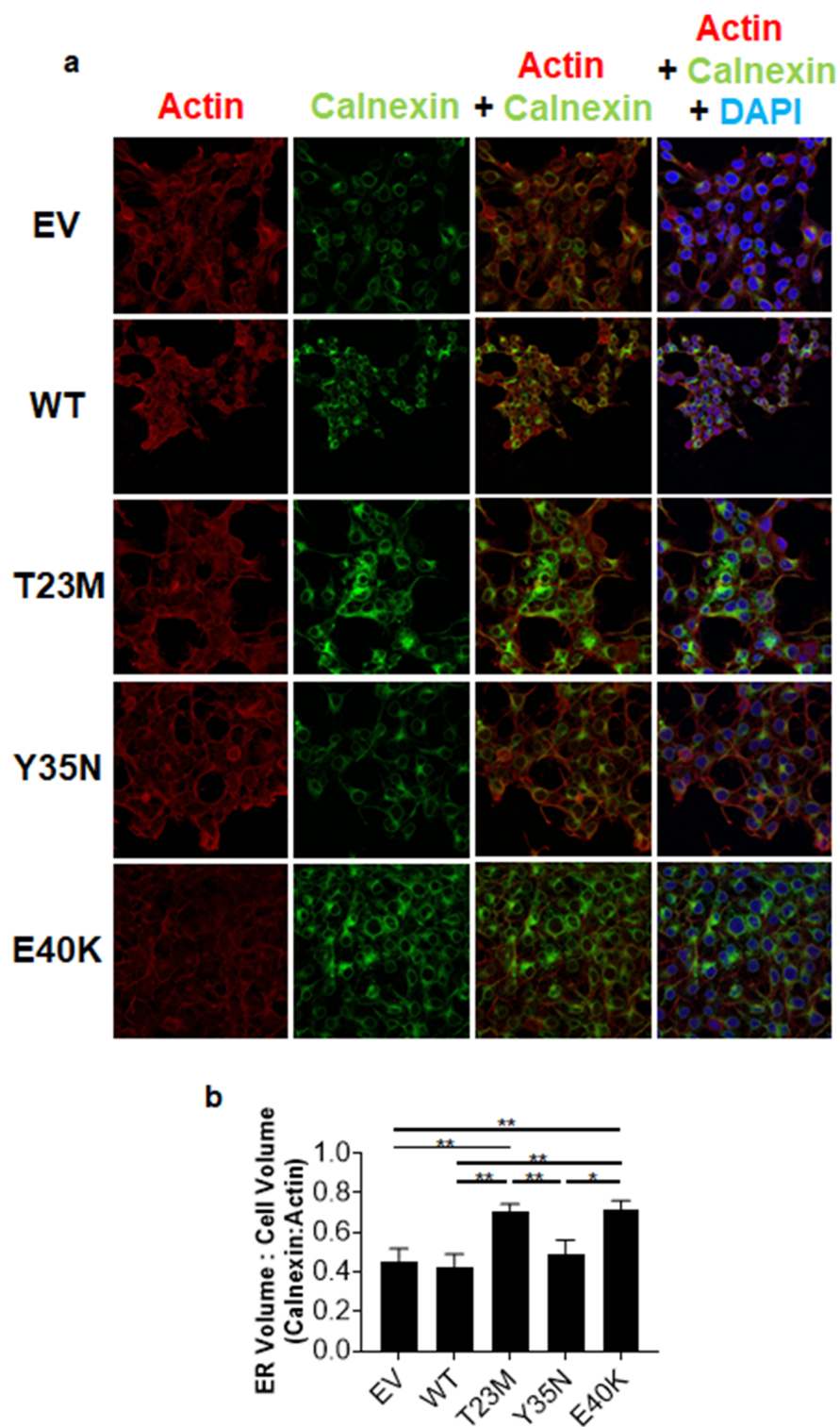


**Figure 2**

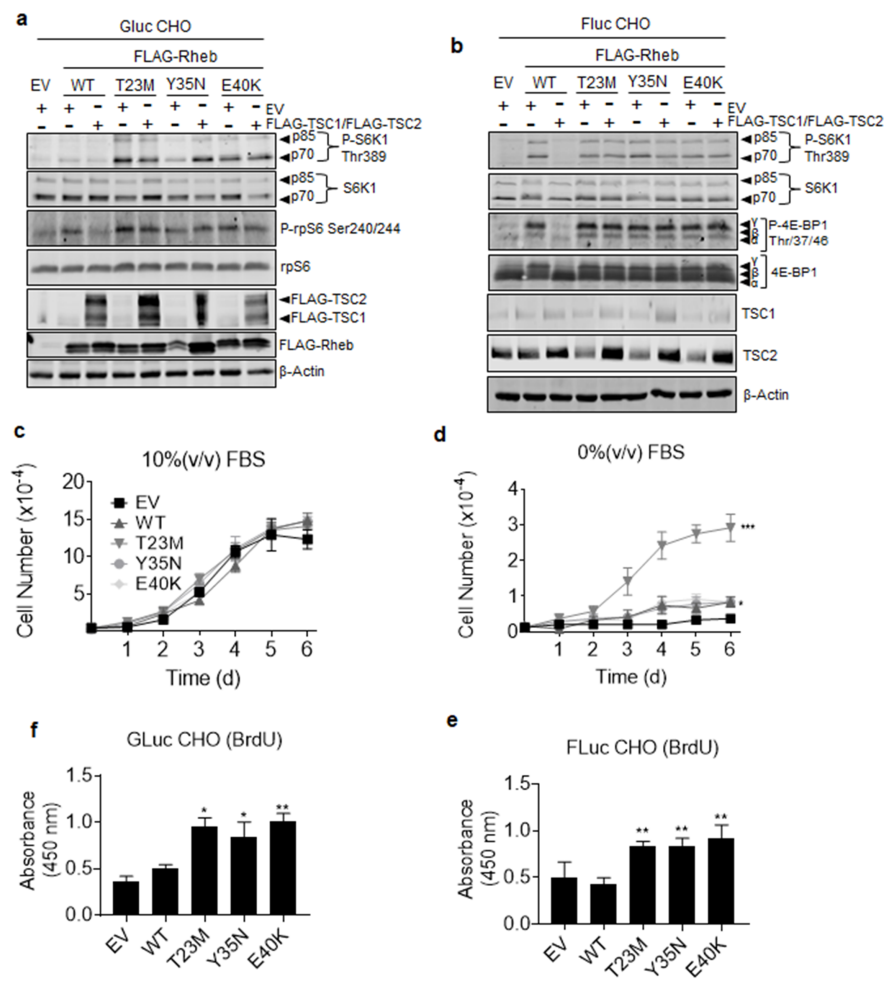


**Figure 3**



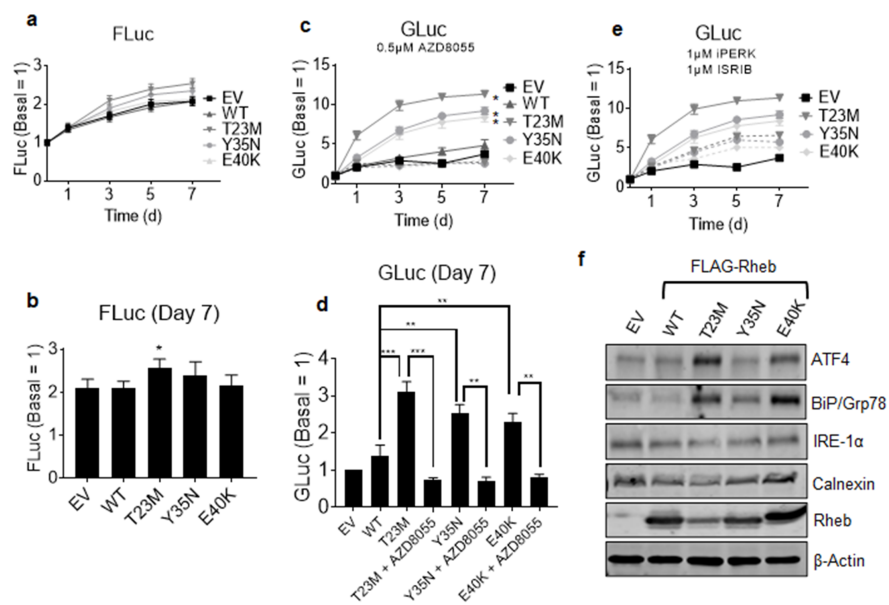


**Figure 4**

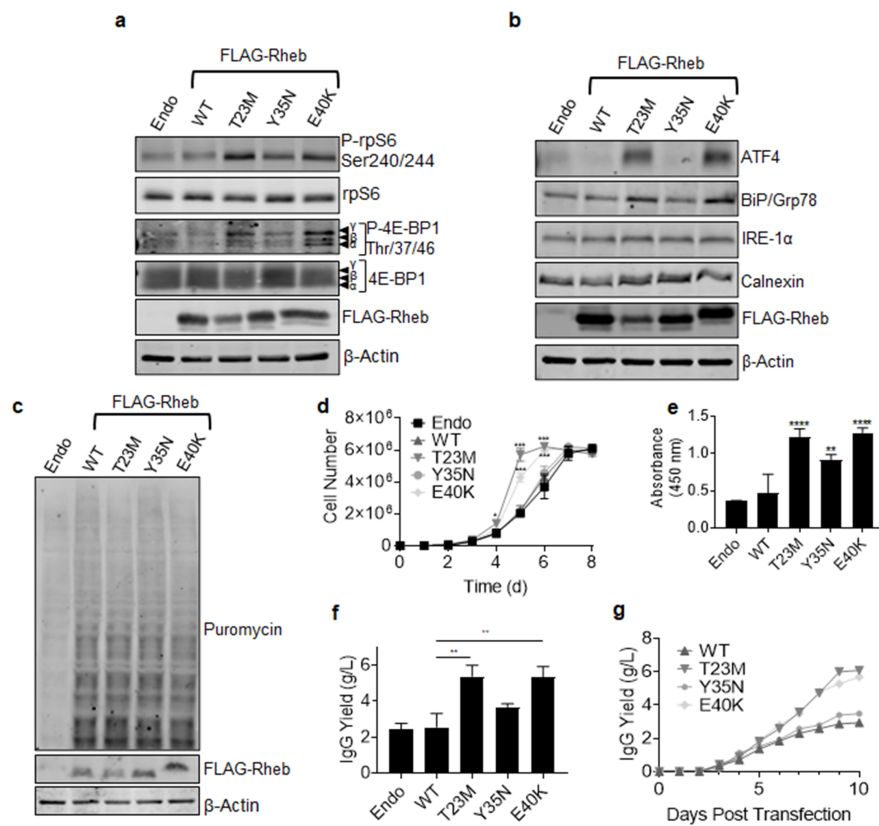


**Figure 5**